Oxygen deficiency and cooling field driven vertical hysteretic shift in epitaxial $SrRuO_3/SrTiO_3$ heterostructures

Ming Zheng,[1,2,a)] Xueyan Li,[3] Wen Xiao,[2] Wei Wang,[4] and Hao Ni[1,5,a)]
[1]*Department of Physics, The University of Hong Kong, Pokfulam Road, Hong Kong*
[2]*Department of Materials Science and Engineering, Faculty of Engineering, National University of Singapore, Singapore 117574, Singapore*
[3]*Department of Materials Science and Engineering, Nanjing University of Science and Technology, Nanjing 210094, China*
[4]*CAS Key Laboratory of Materials for Energy Conversion, Shanghai Institute of Ceramics, Chinese Academy of Sciences, Shanghai 201899, China*
[5]*College of Science, China University of Petroleum, Qingdao 255680, China*

(Received 19 August 2017; accepted 30 September 2017; published online 11 October 2017)

$SrRuO_3$ thin films have been epitaxially grown on $SrTiO_3$ substrates using a pulsed laser deposition technique. By adjusting the oxygen partial pressure during deposition, a sharp drop in the Curie temperature (T_C) of 95 K and vertical magnetization shift (M_{Shift}) of 82.7% in the hysteresis loop was observed due to the oxygen deficiency induced lattice distortion that modifies the strong hybridization of *p-d* orbitals and perpendicular uniaxial magnetic anisotropy. In particular, the vertical hysteretic shift can also be effectively tuned by the applied cooling field, and thus, we obtained a giant and complete M_{Shift} of 106% with a large volume of pinned Ru^{4+} moments. These findings reveal the critical role played by intrinsic oxygen defects and extrinsic cooling field in controlling magnetic couplings in this perovskite-type complex oxide system. *Published by AIP Publishing.*
https://doi.org/10.1063/1.5000866

Perovskite ruthenate $SrRuO_3$ (SRO) has attracted considerable attention for decades due to intriguing physical properties such as metallic conductivity,[1] itinerant ferromagnetism,[2] anomalous Hall effects,[3] magnetocrystalline anisotropy,[4] exchange bias,[5] and vertical magnetization shift[6,7] and promising applications in magnetic tunnel junctions and magnetic random accessory devices.[8–10] Among these striking properties, exchange bias is referred to an offset of the hysteresis loop along the magnetic field axis upon cooling the ferromagnetic-antiferromagnetic system below the ferromagnetic Curie temperature T_C through the antiferromagnetic Neel temperature T_N under an external magnetic field[11] and has garnered perpetual efforts from the scientific community because of its usage in spin valves and magnetic recording media.[12,13] However, the vertical magnetization shift (M_{Shift}), i.e., the offset of the hysteresis loop along the magnetization axis rather than along the field axis, is usually too small and has rarely been detected experimentally. Fortunately, several recent findings on large M_{Shift} have sparked renewed research activity, which offers an additional degree of freedom in future spintronic device applications. For example, Rana *et al.*[14,15] reported that M_{Shift} could be tuned (maximum 36%) by varying the thickness of individual layers in $La_{0.7}Sr_{0.3}FeO_3$/SRO bilayers, exhibiting a proportional (inverse) relationship with the $La_{0.7}Sr_{0.3}FeO_3$ (SRO) layer thickness. This result is attributed to the presence of pinned canted Ru^{4+}/Fe^{3+}-Fe^{5+}moments at the interface and the formation of incomplete domain walls, which can separate the pinned moments from the unpinned moments in the bilayer. In contrast, Singamaneni *et al.*[16] observed a complete M_{Shift} in $La_{0.7}Sr_{0.3}MnO_3$/SRO thin film heterostructures with a thicker (180 nm) SRO layer, which can be interpreted by the strong coupling between the uniaxial magnetocrystalline anisotropy and the interface atomic structure. Moreover, Padhan and Prellier[17] found that M_{Shift} decreases as the $SrMnO_3$ layer thickness increases in $SrMnO_3$/SRO superlattices due to pinned/biased moments in the SRO layer, where the magnetic interaction across the interface is a combination of the exchange coupling between the $SrMnO_3$ layer and the SRO layer and the interlayer exchange coupling between the SRO layers. Despite that most of these studies have focused on the realization and modulation of the large vertical shift in SRO-based superlattices and heterostructures, the M_{Shift} of SRO films is poorly understood and its origin remains debatable. There is no doubt that a systematic investigation of the impacts of both the intrinsic (i.e., stoichiometry and lattice distortion) and extrinsic (i.e., cooling field and temperature) factors on M_{Shift} would help to provide an effective way to control it and elucidate essential physics of SRO films, which opens an avenue for better understanding and improving tunable spintronic devices.

In this work, we grew epitaxial SRO films on $SrTiO_3$ (STO) substrates and robustly modulated the M_{Shift} and T_C of the films by exploiting the growth-induced oxygen deficiencies. We found that M_{Shift} is also strongly dependent on the magnitude and polarity of the cooling field and temperature. These unique physical phenomena are discussed in terms of compositional and strain effects on the hybridization of *p-d* orbitals and perpendicular magnetic anisotropy, as well as the concentration of pinned Ru^{4+} spins.

SRO thin films (~40 nm thick) were fabricated on (001)-oriented STO single-crystal substrates using a pulsed laser deposition technique from a high purity stoichiometric

a)Authors to whom correspondence should be addressed: zhengm@mail.ustc.edu.cn and nihao@upc.edu.cn

SRO ceramic target. The target was ablated using a KrF excimer laser (248 nm) with a pulse energy density of 3 J/cm^2 and a repetition rate of 5 Hz. The growth was carried out at 500 °C under different oxygen pressures (P_{O_2}) of 150 mTorr, 50 mTorr, and 10 mTorr. The as-grown films were annealed *in situ* for 30 min then cooled to room temperature at a rate of 4 °C/min. The crystal structure and in-plane epitaxial relationship between the film and the substrate were examined by the θ-2θ linear scan, ϕ-scan, and reciprocal space mapping using a high-resolution four-circle Bruker D8 Discover X-ray diffractometer (XRD) equipped with Cu $K_{\alpha 1}$ radiation ($\lambda = 1.5406$ Å). The stoichiometry of the film was measured via X-ray photoelectron spectroscopy (XPS). Magnetic data were collected using a SQUID magnetometer (MPMS XL-5, Quantum Design) with the magnetic field applied parallel to the sample plane.

Figure 1(a) shows the XRD θ-2θ scan pattern of the SRO film grown on the STO substrate at P_{O_2}=150 mTorr. Only strong (00l) ($l = 1, 2, 3$) diffraction peaks from the SRO film can be found, indicating that the SRO film is of single phase and highly (001)-oriented (pseudocubic notation). XRD ϕ-scans taken on the SRO(101) and STO(101) diffraction peaks yield two sets of fourfold symmetrical diffraction peaks recurring every 90° at the same azimuthal ϕ-angle [see the left inset of Fig. 1(a)]. This directly describes the epitaxial relationship of $(001)_{SRO}||(001)_{STO}$ and $[100]_{SRO}||[100]_{STO}$, a clear sign of cube-on-cube heteroepitaxy. To check the initial strain state of the SRO film, we performed x-ray reciprocal space mapping around the (−103) diffraction peaks. As presented in the right inset of Fig. 1(a), the reflection from the film appears at the same position as that of the substrate along the in-plane direction (i.e., the horizontal axis), implying that the SRO film is coherently strained. This suggests that the in-plane lattice of the film is clamped by the substrate and the film thus shows a tetragonal structure. The calculated out-of-plane lattice parameter c (∼0.395 nm) of the film is indeed larger than the bulk value (∼0.393 nm),[8] which means that the SRO film suffers an out-of-plane tensile (0.51%) and in-plane compressive (−0.64%) strain.

It is noteworthy that as P_{O_2} is decreased from 150 to 10 mTorr, the SRO(002) reflection shifts to lower 2θ angles and eventually splits from one peak to two peaks [see Fig. 1(b)], disclosing the out-of-plane lattice expansion of the SRO films with reducing oxygen pressure. We accordingly calculated and obtained the out-of-plane lattice parameter c from the out-of-plane θ-2θ scan data [Fig. 1(c)]. Again, as deduced from the reciprocal space mapping, the in-plane lattice parameter a of the films deposited at different oxygen pressures is totally the same as that of the substrate, hinting that all the SRO films are fully strained. It is known that the SRO films grown at low oxygen pressure may produce oxygen deficiencies and introduce charged defects, which would cause an effective unit cell volume expansion to compensate the Coulomb repulsion between the uncompensated charges.[18–20] This volume expansion, together with the in-plane coherent compressive strain, enables the elongation of the c-axis lattice parameter of the film. XPS measurements indeed show that the Ru/O atomic ratio for the SRO films deposited at P_{O_2}=150, 50, and 10 mTorr is estimated to be 1:(2.97 ± 0.05), 1:(2.85 ± 0.05), and 1:(2.65 ± 0.05), respectively, which confirms the oxygen deficiency-induced nature of out-of-plane lattice expansion. To further identify this, all the SRO films were annealed in 1 atm O_2 for 1 h, and finally, they show the same Ru/O atomic ratio as the stoichiometric target. Moreover, the domain size of the SRO film can also be determined from diffraction peak broadening, as shown in Fig. 1(c). One can see that with decreasing P_{O_2} from 150 to 10 mTorr, the domain size is reduced from 28 to 7.5 nm, providing evidence that the larger domain forms in smaller stained films.

Aside from lattice distortion and domain structure, the magnetic properties of the SRO films are also closely related to the growth-induced oxygen deficiencies. Figure 2 shows

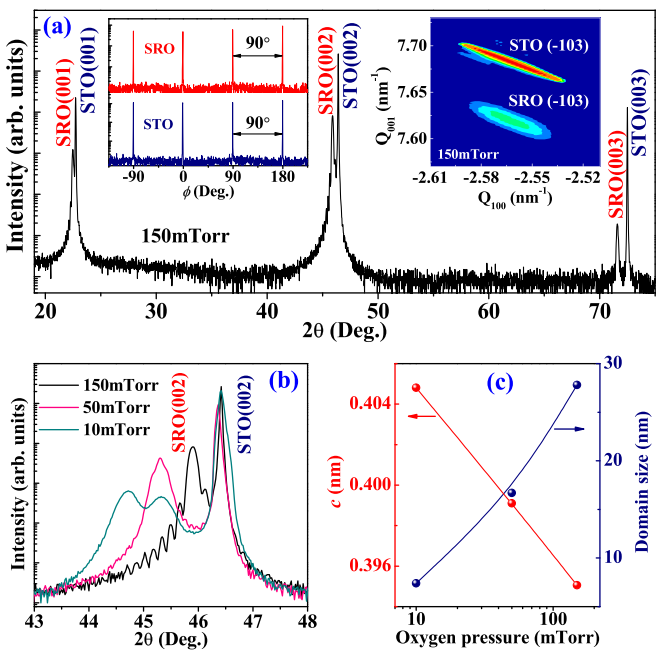

FIG. 1. (a) XRD θ-2θ scan for the SRO film grown on the STO substrate at P_{O_2}=150 mTorr. Left inset: XRD ϕ-scans taken on the SRO(101) and STO(101) diffraction peaks. Right inset: reciprocal space mapping around (−103) diffraction peaks. (b) XRD θ-2θ scans for the SRO films deposited at P_{O_2}=150, 50, and 10 mTorr. (c) The c-axis lattice parameters and domain sizes of SRO films determined from Fig. 1(b).

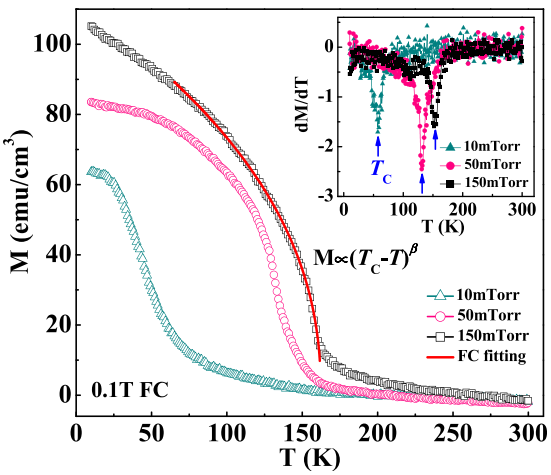

FIG. 2. Temperature dependence of FC magnetization for the SRO films deposited at various oxygen pressures. The red solid line is the fitted result near T_C using the scaling law $M \propto (T_C - T)^{\beta}$. Inset: corresponding d$M$/d$T$ versus T curves.

the temperature dependence of the field-cooled (FC) magnetization for the SRO films deposited under various oxygen pressures. The induced oxygen deficiencies can readily diminish the hybridization strength of Ru 4*d* orbitals and O 2*p* orbitals and suppress the magnetization of the SRO films, which is further corroborated by the magnetic hysteresis loops measured at $T = 10$ and 50 K in Figs. 3 and 4. It has been reported that not only oxygen defects but also the oxygen defect-induced lattice distortion can strongly influence magnetic properties due to the high sensitivity of the magnetic coupling to the interatomic distance.[18,21] Upon reducing P_{O_2} from 150 to 10 mTorr, the *c*-axis lattice parameter of the film is enhanced from 0.395 to 0.4048 nm. The *c*-axis elongated unit cell may disfavor the crossover of the fourth spin of half *d* filled Ru^{4+} ions from the t_{2g} to e_g energy levels owing to the broader energy band gaps, and thus, the high spin configuration of Ru^{4+} ($t_{2g}^{\uparrow\uparrow\uparrow} e_g^{\uparrow}$) ions can be suppressed by the tetragonal distortion.[21] The growth-induced oxygen deficiencies not only merely affect the magnetization but also change the Curie temperature T_C of the SRO films. As can be seen from the dM/dT versus T curves in the inset of Fig. 2, T_C is reduced dramatically from 152 to 57 K with decreasing P_{O_2} from 150 to 10 mTorr. The sharp drop in T_C can be ascribed to the oxygen deficiency-induced weakening of hybridization strength of *d* and *p* orbitals through adjusting the tilts and rotations of octahedra.[18] The inverse proportional of T_C to the *c*-axis lattice parameter suggests that the oxygen deficiency-induced lattice distortion also plays a vital role in the tunability of T_C. The observation of such a significant oxygen deficiency-induced evolution of T_C ($\Delta T_C \sim 95$ K) in SRO films is believed to be unprecedented and demonstrates the effectiveness of oxygen deficiency-manipulation of lattice distortion and electronic structure. Similar to the findings in the SRO bulk and thin films,[22,23] the magnetization data near T_C can be fitted using the scaling law $M \propto (T_C - T)^{\beta}$ [see the red line], where M is the spontaneous magnetization and β is the critical exponent. The β value of the SRO film for P_{O_2}=150 mTorr is ~0.46, close to that (~0.5) of the SRO single crystal,[24] and thus can be reasonably explained on account of the mean field model. Upon decreasing the oxygen pressure, the β value becomes ~0.6 and 0.8 for P_{O_2}=50 and 10 mTorr, respectively. Such disparity in β is probably caused by dissimilar defects, domains, and lattice distortions.[23] These findings explicitly prove that oxygen defect tunable magnetic

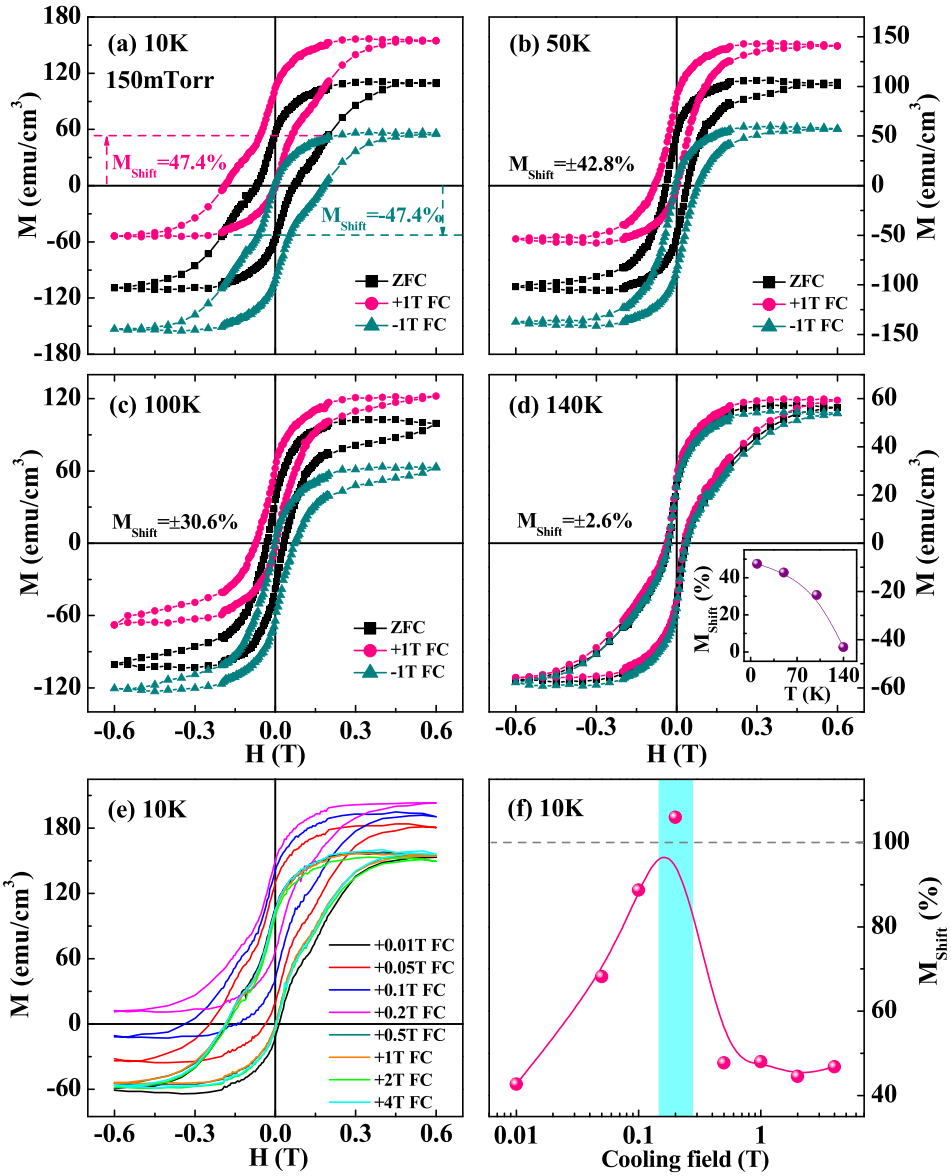

FIG. 3. (a)–(d) Magnetization-magnetic field (*M-H*) hysteresis loops for the SRO film deposited at P_{O_2}=150 mTorr, as measured at $T = 10$, 50, 100, and 140 K after being cooled from $T = 300$ K with and without the application of $H_{CF} = \pm 1$ T, respectively. The inset in Fig. 3(d) shows M_{Shift} as a function of temperature. (e) *M-H* hysteresis loops for the SRO film under various in-plane cooling fields as stated at $T = 10$ K. (f) M_{Shift} as a function of the cooling field at $T = 10$ K.

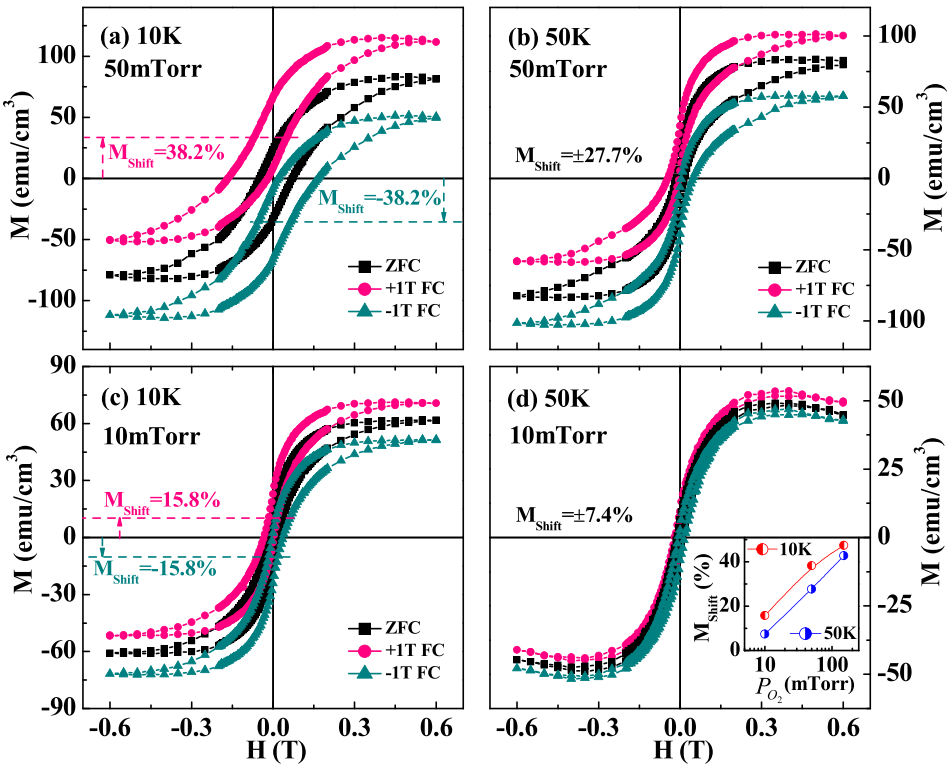

FIG. 4. *M-H* hysteresis loops for the SRO films deposited at $P_{O_2} = 50$ and 10 mTorr, as measured at $T = 10$ and 50 K after being cooled from $T = 300$ K with and without the application of $H_{CF} = \pm 1$ T, respectively. The inset in Fig. 4(d) shows M_{Shift} as a function of oxygen pressure.

properties are microscopically a result of oxygen deficiency-induced lattice distortion.

Figure 3(a) illustrates the magnetization-magnetic field (*M-H*) hysteresis loops for the SRO film deposited at $P_{O_2} = 150$ mTorr, as recoded at $T = 10$ K with and without the application of different signs of cooling field $H_{CF} = \pm 1$ T. Apparently, a symmetrical hysteresis loop centered at the origin was observed in the zero-field-cooled (ZFC) *M-H* curve. Comparatively, the FC hysteresis loops exhibit a remarkable offset along the magnetization axis (M_{Shift}) towards the same sign of the cooling field. This vertical shift can be expressed as $M_{Shift} = [(M^+_{Sat} + M^-_{Sat})/2]/[(M^+_{Sat} - M^-_{Sat})/2]$,[14,15,25] where M^+_{Sat} and M^-_{Sat} are positive and negative saturation values of the hysteresis loop, respectively. M_{Shift} is generally considered to originate from the irreversible pinned spins/moments at the interface while sweeping the magnetic loop.[26] We note before deposition that the STO substrate was annealed at 500 °C under high vacuum with the base pressure less than 10^{-6} mTorr for more than 1 h, which would lead to oxygen loss and the formation of the so-called Ti^{3+}-oxygen vacancy complexes at the upmost surface.[27] During the subsequent growth of SRO films, the highly reactive Ti^{3+} ions at the substrate surface were easily reoxidized to Ti^{4+} ions by reacting with the oxygen atoms of Ru-O precursors, thereby producing a thin Ru^{3+} layer at the film/substrate interface.[28] Consequently, the interfacial antiferromagnetically coupled Ru^{3+} moments act as the pinning center for the pinned Ru^{4+} spins during field cooling through an embedded canted spin layer between them.[29] As depicted in the inset of Fig. 3(d), with increasing temperature from $T = 10$ to 140 K, M_{Shift} is reduced markedly from 47.4% to 2.6%, a decrease of 94.5% indicative of a thermally activated major drop in the pinned moment concentration during heating up. To gain insights into the evolution of the relative fraction of pinned moments against the cooling field, the magnetic hysteresis loops of the SRO film under various cooling fields were measured and shown in Fig. 3(e). We calculated the corresponding M_{Shift} values and presented the results in Fig. 3(f). It is interesting that the cooling field strongly alters M_{Shift}. M_{Shift} initially rises sharply with the increasing cooling field and reaches the maximal value at $H_{CF} = 0.2$ T, before dropping with a further increase in H_{CF}. This evolution of M_{Shift} against H_{CF} reveals that the relative fraction of pinned moments is at its largest at $H_{CF} = 0.2$ T but suppressed when H_{CF} deviates from $H_{CF} = 0.2$ T. Below $H_{CF} = 0.2$ T, the increased cooling field favors the alignment of unpinned moments along the field direction and thus enhances the relative fraction of pinned uncompensated moments after the magnetic loop reversal. Above $H_{CF} = 0.2$ T, the magnetic interaction between the cooling field and the canted spin layer is strong enough so that the coupling of the pinned Ru^{4+} moments and the canted spin layer is frustrated,[29] giving rise to the suppression of the pinning effect. As a result, $H_{CF} = 0.2$ T can be identified as an effective depinning threshold field,[30] above which the pinned canted spins/moments can be rotatable and gradually become unpinned. These magnetic data conspicuously establish that M_{Shift} is strongly coupled to the cooling field and temperature.

To probe into the oxygen deficiency dependence of the vertical magnetization shift, we also conducted magnetic hysteresis loop measurements for the SRO films deposited at $P_{O_2} = 50$ and 10 mTorr, as shown in Figs. 4(a)–4(d). Upon decreasing P_{O_2} from 150 to 10 mTorr, M_{Shift} at any fixed temperature (e.g., $T = 10$ and 50 K) is effectively suppressed [see the inset of Fig. 4(d)]. For example, M_{Shift} at $T = 50$ K decreases from 42.8% for $P_{O_2} = 150$ mTorr to 7.4% for $P_{O_2} = 10$ mTorr, a reduction of 82.7%. The oxygen deficiencies can change the orientation of the RuO_6 octahedra and modify

the spin-orbit coupling, thus tuning the M_{Shift} of the films. Moreover, it has been demonstrated that the pseudocubic SRO films show in-plane uniaxial magnetic anisotropy, whereas the tetragonal films possess perpendicular uniaxial magnetic anisotropy.[19,20] With reducing oxygen pressure, the *c*-axis lattice parameter of the tetragonal SRO films increases, displaying more significant perpendicular uniaxial magnetic anisotropy. The applied in-plane cooling field disfavors the alignment of unpinned moments along the field direction, and hence, the relative fraction of in-plane pinned uncompensated moments was diminished after sweeping the hysteresis loop. Therefore, the oxygen deficiency-induced lattice distortion mediated magnetic anisotropy contributes to the large evolution of M_{Shift}. In addition, more domain boundaries could be generated at low oxygen pressure, which weakens the alignment of unpinned Ru^{4+} moments along the field direction during the field cooling and suppresses M_{Shift}. Based on this, it is assumed that the oxygen defect-induced change in lattice strain and domain structure is essentially responsible for the tunable vertical hysteretic shift. It should be noted that besides the oxygen deficiencies, Ru deficiencies could also drastically affect the structural and physical properties of SRO films.[31,32] We ever reported that Ru deficiencies could be formed by reducing the oxygen partial pressure, followed by annealing *in situ* in 1 atm O_2 to rule out oxygen deficiencies.[33] The low-pressure grown SRO film showed a higher vertical hysteretic shift,[33] which is at odds with our observation here that the low-pressure grown film exhibited a lower vertical shift. Such a difference could be attributed to the different type of the deficiencies formed in the films. In this work, the SRO films were grown at a relatively low temperature of 500 °C (lower than 690 °C in Ref. 33) without annealing in 1 atm O_2. The presence of ruthenium or oxygen deficiencies is sensitive to the growth condition (e.g., deposition temperature and annealing treatment), as previously reported by Lu *et al.*[19,20]

In summary, we reported the coherent epitaxial growth of SRO films on STO substrates and realized the unprecedented oxygen deficiency-induced variation of magnetic properties. Upon reducing oxygen pressure, the growth-induced oxygen deficiencies enable the elongation of the *c*-axis lattice parameter and the reduction of the domain size of the films, which results in the dramatic suppression of Curie temperature ($\Delta T_C \sim 95$ K) and vertical hysteretic shift ($\Delta M_{Shift}/M_{Shift} \sim 82.7\%$). We attribute these fascinating physical phenomena to oxygen defect-induced structural distortion and the resultant change in the hybridization strength of Ru 4*d* and O 2*p* orbitals and perpendicular uniaxial magnetic anisotropy. Particularly, an appreciable and complete ($M_{Shift} > 100\%$) vertical hysteretic shift was achieved by selecting the cooling field to adjust the relative fraction of pinned Ru^{4+} moments. This work opens an effective gate to tune the Curie temperature and vertical hysteretic shift of the SRO films by intrinsic oxygen defects and extrinsic cooling field.

This work was supported by the National Natural Science Foundation of China (Grant No. 11504432), the Shandong Provincial Natural Science Foundation (Grant No. BS2015DX002), and the Qingdao Science and Technology Program for Youth (Grant No. 16-5-1-6-jch).

[1]C. B. Eom, R. J. Cava, R. M. Fleming, J. M. Phillips, R. B. Vandover, J. H. Marshall, J. W. P. Hsu, J. J. Krajewski, and W. F. Peck, Science **258**, 1766 (1992).
[2]L. Klein, J. R. Reiner, T. H. Geballe, M. R. Beasley, and A. Kapitulnik, Phys. Rev. B **61**, R7842 (2000).
[3]Z. Fang, N. Nagaosa, K. S. Takahashi, A. Asamitsu, R. Mathieu, T. Ogasawara, H. Yamada, M. Kawasaki, Y. Tokura, and K. Terakura, Science **302**, 92 (2003).
[4]X. W. Wang, Y. Q. Zhang, H. Meng, Z. J. Wang, D. Li, and Z. D. Zhang, J. Appl. Phys. **109**, 07D707 (2011).
[5]C. Sow, A. K. Pramanik, and P. S. Anil Kumar, J. Appl. Phys. **116**, 194310 (2014).
[6]L. Pi, S. X. Zhang, S. Tan, and Y. H. Zhang, Appl. Phys. Lett. **88**, 102502 (2006).
[7]L. Klein, Appl. Phys. Lett. **89**, 036101 (2006).
[8]D. C. Worledge and T. H. Geballe, Phys. Rev. Lett. **85**, 5182 (2000).
[9]K. S. Takahashi, A. Sawa, Y. Ishii, H. Akoh, M. Kawasaki, and Y. Tokura, Phys. Rev. B **67**, 094413 (2003).
[10]G. Koster, L. Klein, W. Siemons, G. Rijnders, J. S. Dodge, C. B. Eom, D. H. A. Blank, and M. R. Beasley, Rev. Mod. Phys. **84**, 253 (2012).
[11]J. Nogues, J. Sort, V. Langlais, V. Skumryev, S. Surinach, J. S. Munoz, and M. D. Baro, Phys. Rep. **422**, 65 (2005).
[12]M. Bibes, J. E. Villegas, and A. Barthelemy, Adv. Phys. **60**, 5 (2011).
[13]B. Dieny, V. S. Speriosu, S. S. P. Parkin, B. A. Gurney, D. R. Wilhoit, and D. Mauri, Phys. Rev. B **43**, 1297 (1991).
[14]R. Rana, P. Pandey, and D. S. Rana, Appl. Phys. Lett. **104**, 092413 (2014).
[15]R. Rana, P. Pandey, R. P. Singh, and D. S. Rana, Sci. Rep. **4**, 4138 (2014).
[16]S. R. Singamaneni, W. Fan, J. T. Prater, and J. Narayan, J. Appl. Phys. **117**, 17B711 (2015).
[17]P. Padhan and W. Prellier, Phys. Rev. B **72**, 104416 (2005).
[18]Y. J. Chang, J. I. Kim, and C. U. Jung, J. Magn. **13**, 61 (2008).
[19]W. L. Lu, W. D. Song, K. H. He, J. W. Chai, C. J. Sun, G. M. Chow, and J. S. Chen, J. Appl. Phys. **113**, 063901 (2013).
[20]W. L. Lu, P. Yang, W. D. Song, G. M. Chow, and J. S. Chen, Phys. Rev. B **88**, 214115 (2013).
[21]M. Bohra, C. P. Wu, H. J. Yeh, Y. H. Cheng, C. C. Peng, and H. Chou, J. Appl. Phys. **109**, 07D728 (2011).
[22]R. Palai, H. Huhtinen, J. F. Scott, and R. S. Katiyar, Phys. Rev. B **79**, 104413 (2009).
[23]C. Sow, D. Samal, P. S. Anil Kumar, A. K. Bera, and S. M. Yusuf, Phys. Rev. B **85**, 224426 (2012).
[24]D. Kim, B. L. Zink, F. Hellman, S. McCall, G. Cao, and J. E. Crow, Phys. Rev. B **67**, 100406(R) (2003).
[25]S. J. Yuan, L. Li, T. F. Qi, L. E. DeLong, and G. Cao, Phys. Rev. B **88**, 024413 (2013).
[26]H. Ohldag, A. Scholl, F. Nolting, E. Arenholz, S. Maat, A. T. Young, M. Carey, and J. Stöhr, Phys. Rev. Lett. **91**, 017203 (2003).
[27]Q. X. Zhu, M. Zheng, M. M. Yang, R. K. Zheng, Y. Wang, X. M. Li, and X. Shi, Appl. Phys. Lett. **105**, 241604 (2014).
[28]S. Vasala and M. Karppinen, Prog. Solid State Chem. **43**, 1 (2015).
[29]A. P. Chen, Q. Wang, M. R. Fitzsimmons, E. Enriquez, M. Weigand, Z. Harrell, B. McFarland, X. J. Lü, P. Dowden, J. L. MacManus-Driscoll, D. Yarotski, and Q. X. Jia, Adv. Mater. **29**, 1700672 (2017).
[30]L. Del Bianco, D. Fiorani, A. M. Testa, E. Bonetti, and L. Signorini, Phys. Rev. B **70**, 052401 (2004).
[31]B. Dabrowski, O. Chmaissem, P. W. Klamut, S. Kolesnik, M. Maxwell, J. Mais, Y. Ito, and B. D. Armstrong, Phys. Rev. B **70**, 014423 (2004).
[32]W. Siemons, G. Koster, A. Vailionis, H. Yamamoto, D. H. A. Blank, and M. R. Beasley, Phys. Rev. B **76**, 075126 (2007).
[33]M. Zheng and W. Wang, ACS Appl. Mater. Interfaces **8**, 14012 (2016).